Extremely High-Speed GaAs Growth by MOVPE for Low-Cost PV Application

Hassanet Sodabanlu ⬤, Akinori Ubukata, Kentaroh Watanabe, Takeyoshi Sugaya,
Yoshiaki Nakano, *Member, IEEE*, and Masakazu Sugiyama

Abstract—Epitaxial growth of GaAs in a horizontal metalorganic vapor phase epitaxy reactor was investigated to realize ultrafast growth rate, which has been demonstrated to be 90 μm/h at maximum. The GaAs growth rate had more or less a linear relationship with the amount of trimethylgallium supply. With extremely fast deposition >70 μm/h, slight saturation of growth rate was observed, which is most likely due to parasitic gas-phase reactions and/or limitation in bubbling. The impact of growth rates was examined using GaAs p-n solar cells, with the 2-μm-thick n-GaAs base layers grown at 20, 60, and 80 μm/h. The studies have not evidenced a significant change in performance as a function of growth rate. The base thickness was expanded to 3.5 μm with the growth rate of 80 μm/h to increase light absorption. The growth rate of 80 μm/h did not induce significant degradation in the efficiency of the cells as compared with the ones grown at 20 and 60 μm/h. The average efficiency of 23.6% (16.3% on the basis of a mesa area) under AM1.5G was realized in the cells with 3.5-μm-thick bases grown at 80 μm/h.

Index Terms—III–V semiconductor materials, photovoltaic cells, semiconductor growth.

I. INTRODUCTION

THE III–V multiple junction solar cells (MJSCs) have been a focus of attention for high conversion efficiency [1]–[3]. Recently, a record efficiency of 46% has been achieved by 4-junction structure under concentration light of 508 sun [4]. Their high cost-performance ratio has restricted the uses of MJSCs to certain applications, notably in the areas of space applications [5], [6]. For terrestrial application, MJSCs in concentrator photovoltaics [7]–[9] have been emerging with a rapid increase of worldwide installation. Generally, there are two approaches for improving cost-performance ratio, namely increasing a cell performance and reducing a cell cost. As for the first approach, a conversion efficiency of MJSCs can be improved by utilizing more p-n junctions to lower the thermalization loss [10], [11] and by balancing the photocurrent generated in each subcell [12], [13]. On the other hand, considerable efforts are recently being focused on the reduction of production costs of MJSCs. Epitaxial lift-off [14], wafer reuse, and high-speed crystal growth by metalorganic vapor phase epitaxy (MOVPE) [15], [16] are considered promising means for achieving this. Results of price per watt analysis show that the reduction in the overhead time of MOVPE reactors, together with the improvement in material utilization efficiency, can reduce the cost of GaAs single junction solar cells by 74%, when the growth rate of GaAs is boosted from 14 to 56 μm/h with performance loss less than 1% [16]. A very recent publication from the same research group presented the detailed analysis of GaAs solar cells grown at high growth rates [17]. The study reported only 0.8% degradation of absolute efficiency when the growth rate was accelerated from 14 to 60 μm/h.

In this paper, we studied the feasibility of MOVPE for realizing extremely high-speed growth, mainly for GaAs solar cell applications. The growth rate of GaAs was boosted to 90 μm/h, which is the maximum growth rate which can be realized with the current reactor design and capability of mass flow controllers. The crystal quality of epitaxial GaAs layers was examined to optimize the growth conditions. The performance of GaAs p-n solar cells, the thick base layer of which was grown at various growth rates, serves as an indicator of the quality of epitaxial GaAs.

II. EXPERIMENTAL DETAILS

The epitaxial growth in this paper was carried out using a horizontal MOVPE reactor (Taiyo Nippon Sanso, HR3335). The reactor was designed to satisfy the requirements for fast chemical reactions and mass transport of highly concentrated gas precursors. Standard sources were utilized with H_2 carrier gas, including trimethylgallium (TMGa), trimethylindium, arsine (AsH_3), phosphine (PH_3), disilane (Si_2H_6), and diethylzinc. Two TMGa bubblers were installed in this system; one for high-speed growth ($\geq$20 μm/h) and the other for normal growth rate. The experiment of GaAs growth was initially conducted with standard growth conditions: reactor pressure (P_g), growth temperature (T_g) and V/III ratio of 10 kPa, 650 °C and 20,

H. Sodabanlu, K. Watanabe, and M. Sugiyama are with the Research Center for Advanced Science and Technology, The University of Tokyo, Tokyo 153-8904, Japan (e-mail: sodabanlu@hotaka.t.u-tokyo.ac.jp; kentaroh@hotaka.t.u-tokyo.ac.jp; sugiyama@ee.t.u-tokyo.ac.jp).

A. Ubukata is with the Taiyo Nippon Sanso Corporation, Tsukuba 300-2611, Japan (e-mail: Akinori.Ubukata@tn-sanso.co.jp).

T. Sugaya is with the Research Center for Photovoltaics, National Institute of Advanced Industrial Science and Technology, Tsukuba 305-8568, Japan (e-mail: t.sugaya@aist.go.jp).

Y. Nakano is with the Department of Electrical Engineering and Informatics Systems, The University of Tokyo, Tokyo 113-8656, Japan (e-mail: nakano@rcast.u-tokyo.ac.jp).

Color versions of one or more of the figures in this paper are available online at http://ieeexplore.ieee.org.

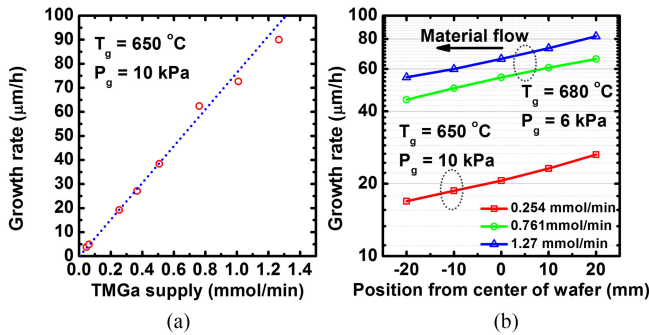Digital Object Identifier 10.1109/JPHOTOV.2018.2814919

Fig. 1. (a) Dependence of GaAs growth rate on TMGa supply at reactor temperature of 650 °C and pressure of 10 kPa. (b) Distribution of GaAs growth rate along material flow direction without wafer rotation using various TMGa supply rates.

Fig. 2. Surface morphologies of 4-μm-thick undoped GaAs layers grown on (100) just GaAs substrates with deposition rate of 20, 60 and 90 μm/h using various growth conditions: growth temperature of 650 °C and 680 °C, reactor pressure of 6 and 10 kPa. The V/III ratio utilized during the growth was 20, for all the growth rates.

respectively. GaAs substrates were used with (100) just surface or vicinal (100) surface (2° off toward (011)). The growth rates of GaAs with various TMGa supplies were evaluated by the thickness of epitaxial layers measured by cross-sectional scanning electron microscope (SEM) images. Atomic force microscopy (AFM) measurement was employed to examine the surface morphology of epitaxial layers. Growth conditions such as temperature and pressure were optimized to realize good GaAs layers. Free carrier concentrations were evaluated by electrochemical capacitance-voltage (ECV) method for optimizing growth parameters of Si- and Zn-doped GaAs grown at various deposition rates. After that, GaAs p-n solar cells were fabricated, for which the 2-μm-thick n-GaAs base layer was grown at various speeds of 20, 60, and 90 μm/h. For the growth of PV structure, Si-doped ($1-2 \times 10^{18}$ cm^{-3}) GaAs (100) wafers, oriented 2° off toward (011), were utilized. The current–voltage (I–V) characteristic under AM1.5G (100 mW/cm^2) illumination and the external quantum efficiency (EQE) spectrum of each solar cell without and with ZnS/SiO$_2$ antireflection coating (ARC) were evaluated and statistically compared. To demonstrate the potentials of high-speed growth and to benchmark the quality of epitaxial layers grown in this reactor, a p-n solar cell with a 3.5-μm-thick n-GaAs base was also fabricated using the fastest growth rate. Cross-sectional SEM images of all PV cells were also taken to evaluate the actual thickness and growth rate of the base layer.

III. RESULTS AND DISCUSSION

A. High-Speed GaAs Growth

It is generally known that the diffusion of precursor fluxes from the gas phase through the mass-transport boundary layer limits the growth rate of GaAs in an ordinary MOVPE reactor [18]. Therefore, in this paper, the MOVPE reactor was designed to have a larger amount of precursor fluxes arriving at substrates by decreasing the thickness of the boundary layer. By reducing the channel height of the flow liner in the reactor, the mass transfer of precursors to the wafer surface was enhanced, resulting in a faster growth rate. Under the standard growth conditions, the GaAs growth rates are plotted as a function of TMGa supply in Fig. 1(a). A good linear relationship can be clearly observed. A
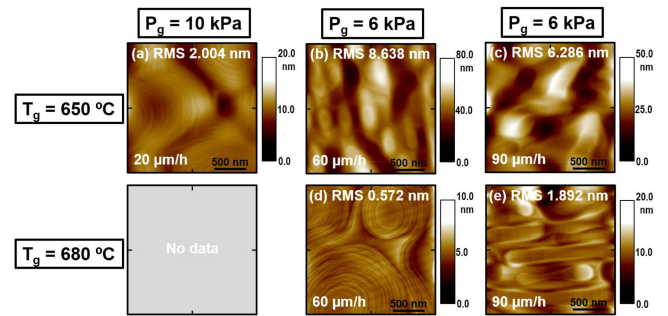
slight saturation of this tendency exists for growth rates faster than 70 μm/h. The most likely explanation may be the parasitic gas-phase reactions, which form GaAs-related particles and reduce the incorporation of precursors to the solid GaAs [19], [20]. In addition, the molar output of TMGa from the bubbler can deviate from proportionality with carrier gas flow when the flow rate is too high, which may be one reason for this growth rate saturation [21], [22]. The steady decay of GaAs growth rate along the material flow direction was seen in this particular MOVPE reactor when wafer rotation was stopped, as shown in Fig. 1(b). The gas phase depletion rate of TMGa was found to be independent of material flow velocities of about 170 and 280 cm/s for the reactor pressures of 10 and 6 kPa, respectively. The flow velocity of gas, parallel to the laminar horizontal reactor, was calculated by the total amount of gas supply passing through the cross-sectional area of the reactor.

The surface morphologies were examined by AFM and shown in Fig. 2(a)–(e) for an area of 2×2 μm^2 of 4-μm-thick undoped GaAs layers deposited with various growth conditions on GaAs (100) just substrates. The V/III ratio utilized during the growth was 20 for all the deposition rates. For Fig. 2(a), in the case of 20 μm/h, the GaAs layer was grown using the standard growth conditions, $P_g = 10$ kPa and $T_g = 650$ °C. Small GaAs islands and clusters with step-terrace structure indicated that the surface migration of group III adatoms was not sufficient. The effect of reactor pressure on the growth mechanism was investigated, and it was found that a lower pressure could be beneficial for better surface migration, resulting in better GaAs morphology. Therefore, the growths of GaAs with larger growth rates of 60 and 90 μm/h were conducted under a low reactor pressure of 6 kPa, and the AFM results are shown in Fig. 2(b) and (c), respectively. The previous study in [17] suggests that a higher growth temperature can improve the mobility of adatoms, resulting in a lower defect density in GaAs and a better solar cell performance. This is in accordance with the studies from Hurle [23] and Schulte and Kuech [24] showing that deep level EL2 defects in GaAs can be reduced with a higher growth temperature. In this paper, we also observed that the surface migration of adatoms could be enhanced by increasing the growth temperature. Fig. 2(d) and (e) show the noticeable improvements of GaAs surface roughness when the growth temperature was in-
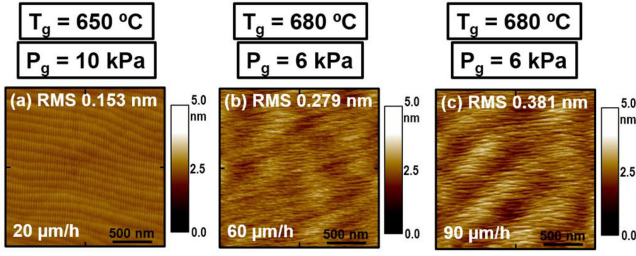
Fig. 3. Surface morphologies of (a) 20, (b) 60, and (c) 90 μm/h grown 4-μm-thick undoped GaAs layers with optimized growth conditions on vicinal GaAs substrates (2° off toward (011)). The V/III ratio during the growth of GaAs on was 20 for all the growth rates.
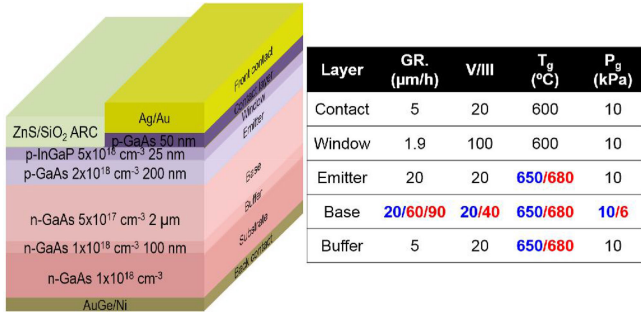

Layer	GR. (μm/h)	V/III	T_g (°C)	P_g (kPa)
Contact	5	20	600	10
Window	1.9	100	600	10
Emitter	20	20	650/680	10
Base	20/60/90	20/40	650/680	10/6
Buffer	5	20	650/680	10

Fig. 4. Design of GaAs p-n solar cells and growth conditions of each layers. The V/III ratio and the growth temperature were 20 and 650 °C, respectively, for growth rate of 20 μm/h. In case of 60 and 90 μm/h growth rate, the V/III ratio and the growth temperature were increased to 40 °C and 680 °C, respectively.

creased from 650 °C to 680 °C for 60 and 90 μm/h growth rates, respectively. In this study, the most remarkable improvement in the GaAs surface morphology grown at extremely high rate was realized by employing GaAs substrates with vicinal (100) surface (2° off toward (011)). Following these strategies, high growth temperature, low reactor pressure, and vicinal substrates, 4-μm-thick undoped GaAs layers with excellent crystal quality and surface morphology were obtained with growth rates of 20, 60, and 90 μm/h, as shown in Fig. 3(a)–(c), respectively. The V/III ratio during the growth of GaAs here was 20 for all the growth rates. The RMS roughness of the GaAs surface could be reduced to less than 0.4 nm. Hence, the fabrication of GaAs p-n solar cells, the structure of which is depicted in Fig. 4, could be carried out, neglecting the influences of GaAs surface morphology.

B. Fabrication of GaAs p-n Solar Cells

The design of GaAs p-n solar cells in this study comprised a 2-μm-thick n-GaAs base layer grown at various rates: 20, 60, and 90 μm/h on the basis of the growth conditions obtained from Fig. 1(a). The growth temperature and V/III ratio for 60 and 90 μm/h growth rates were increased to 680 °C and 40, respectively. In this paper, to ensure the quality of high-speed grown GaAs, a high V/III ratio of 40 was utilized. The impact of V/III ratio will be investigated in future work. The growth rate of p-GaAs emitter layer was kept constant at 20 μm/h to emphasize the effects of growth rate of 2-μm-thick base layer on the performance of p-n solar cells. In addition, to shorten the

growth recipes and to avoid exposing the n-GaAs surface, i.e., junction interface, during temperature stabilization, the reactor temperature for GaAs was constantly maintained at 680 °C for the growth of the 60 and 90 μm/h samples. In this study, the InGaP window layers were Ga-rich (approximately 60% Ga composition) to decrease light absorption and to increase the band offset. No back-surface-filed (BSF) heterolayer was employed in this structure, but only highly doped GaAs buffer layer was grown prior to the n-GaAs base. The reason is the ease of growth, since the gas switching between As and P has not been fully investigated and optimized yet. The growth parameters of each layer are summarized in the table of Fig. 4. Some values are highlighted with either blue or red colors to clarify the different growth conditions for 20 μm/h (blue) and for 60 and 90 μm/h growth rates (red). Each GaAs p-n wafer grown at various rates was fabricated into 28 cells, the mesa area of which was defined to be 0.047 cm^2 using a photolithography mask. AuGe/Ni and Ag/Au metals were deposited for ohmic contacts with n- and p-GaAs, respectively. The front electrode covers about 31.9% of mesa area, corresponding to an effective cell area of 0.032 cm^2. After etching the p-GaAs contact layers, PV characteristics of each sample were measured. Then, the samples were deposited with ZnS/SiO$_2$ ARC by sputtering method to decrease surface reflectance, and the *I–V* and EQE measurements were repeated. The growth conditions, the fabrication procedures and the measurement methods of the solar cell with 3.5-μm-thick base layer, grown at the fastest growth rate, were identical with those of the samples with the 2-μm-thick base. The thickness of the base layer was controlled by adjusting the growth time.

As aforementioned, the growth parameters were adjusted for each growth rate to obtain good GaAs epitaxial layers. Therefore, prior to the growth of GaAs p-n solar cells, the doping conditions, especially for Si-doped GaAs, were investigated and optimized. The sample structure for this experiment consisted of four to five layers of n-GaAs doped with various supplies of Si$_2$H$_6$. The V/III ratio, temperature, and reactor pressure of each growth rate were similar to the growth conditions of the n-GaAs base as summarized in Fig. 1. Free electron concentrations in the Si-doped GaAs layer were measured by the ECV method, and plotted as functions of molar flow ratio between of Si$_2$H$_6$ and TMGa in Fig. 5. Linear dependences between free carrier and dopant concentrations were obtained for each growth rate. It seems that Si incorporation efficiency did not depend on the GaAs growth rate, indicating a linear increase of dopant incorporation rate with the amount of supplied precursors. To evaluate the background doping concentration of each growth rate, unintentionally doped 4-μm-thick GaAs layers were grown on GaAs (100) just substrates using the growth conditions (P_g, T_g, V/III ratio) of the n-GaAs base layer. The background hole concentrations were approximately 1.6×10^{15}, 7.1×10^{15}, and 1.4×10^{16} cm^{-3} for the 20, 60, and 90 μm/h growth rates, respectively, which were much less than the electron concentration in the n-GaAs base layer in the solar cell design. This background hole doping can be potentially ascribed to either background carbon impurity or acceptor-type defects. It is generally known that a higher V/III ratio and a higher growth temperature lead to a lower carbon incorporation in MOVPE grown
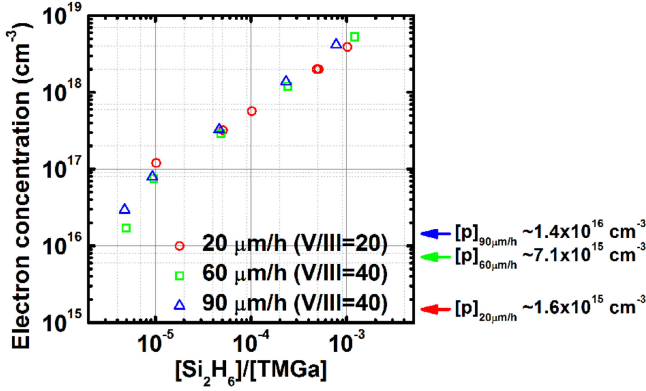
Fig. 5. Dependences of free electron concentration in Si-doped GaAs layers on the ratio between molar flows of Si_2H_6 and TMGa. The background hole concentrations of each growth rate are given next to the graph.

TABLE I
THICKNESS AND ACTUAL GROWTH RATE (GR) OF BASE
LAYER OF GaAs p-n SOLAR CELLS

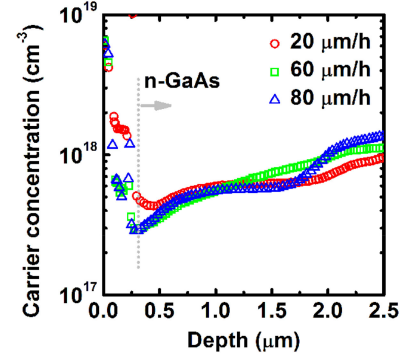| Designated GR (μm/h)	Designated base thickness (μm)	Measured base thickness (μm)	Actual GR (μm/h)
20	2	2.01	20
60	2	2.00	60
90	2	1.69	76
90	4	3.54	80

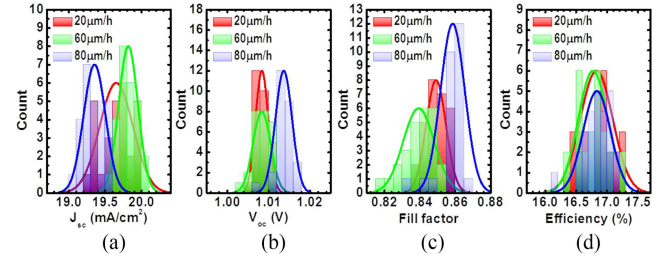Fig. 6. Profiles of carrier concentration in the GaAs p-n solar cells growth with various growth rates.

Fig. 7. Distribution of (a) J_{sc}, (b) V_{oc}, (c) efficiency, and (d) fill factor under AM1.5G illumination of GaAs p-n solar cells grown with various deposition rates without ZnS/SiO$_2$ ARC evaluated using the effective area of 0.032 cm^2.

GaAs using TMGa and AsH$_3$ [25]–[27], and the growth rate has almost no effect on the background carbon level. However, it is still possible that excessively high growth rate impedes the elimination of carbon from the surface of GaAs, which is believed to proceed via the reaction between methyl adsorbates and As-H complexes on the GaAs surface [25]–[27]. Hence, GaAs growth rate can possibly influence background carbon concentrations at extremely high growth rates. MOVPE grown GaAs layers under As rich (high V/III ratio) condition generally contain As antisites, As interstitials, and Ga vacancies, which are donor type defects [17], [28]. Ga antisites, double accepter defects, does not seem to be a reason of this background hole doping. Secondary-ion mass spectrometry and deep-level transient spectroscopy can clarify this issue of background doping further, but here we just compensate the background doping and try to evaluate the performance of PV cells. According to these ECV results, the electron concentration in the n-GaAs base layer grown at different rates can be controlled satisfactorily.

The thickness and actual growth rate of the base layers were evaluated by cross-sectional SEM images and summarized in Table I. We found that the growth condition changed by approximately 10% only for the 90 μm/h growth; actual growth rate was 80 μm/h. This might be due to incomplete saturation of TMGa vapor in the bubbler when the liquid level is low (close to depletion of TMGa in the bubbler), which was the case when a series of the cells was fabricated. From this point onward, the growth rate of 90 μm/h for GaAs cells will be corrected to 80 μm/h on the basis of this finding.

Fig. 6 shows the profiles of carrier concentration in the GaAs p-n solar cells with 2-μm thick bases. There are several remarkable discussion points for this graph. Having a good agreement with SEM images, the sample grown with 80 μm/h speed had a slightly thinner base layer than the designated value of 2 μm, as shown in the blue-dot plot. From the ECV profiles, the carrier concentration in Zn-doped layers of the 60 and 80 μm/h grown samples was noticeably smaller than that of the 20 μm/h grown sample. The reason is that growth conditions of Zn-doped GaAs emitter were not calibrated at 680 °C, and the incorporation of Zn atoms could be affected by growth temperature. Moreover, at around the interface between p-GaAs and n-GaAs, the carrier concentrations of the 60 and 80 μm/h grown samples was slightly smaller than that of the 20 μm/h one. The n-doping in the base layer might be compensated by the thermal diffusion of Zn atoms at the higher growth temperature. Owing to the previous experiment of Si doping, the electron concentrations in the n-GaAs base layer of each sample were excellently controlled to be approximately 5×10^{17} cm^{-3}. The 60 μm/h grown sample had a slightly different carrier profile in this n-GaAs region, most likely due to an artifact in the measurement: nonuniform etching during ECV measurement. Lastly, there is a slight deviation of the doping concentration in the n-GaAs substrates, possibly because of different substrate lots and the artifact in the measurement.

C. GaAs Cell Performance and the Effects of Growth Rate

Fig. 7(a)–(d) show the distribution of short-circuit current density (J_{sc}), open-circuit voltage (V_{oc}), fill factor (FF), and conversion efficiency (η), respectively, under AM1.5G illumination for the GaAs solar cells (based on the effective area

TABLE II
AVERAGE AND STANDARD DEVIATION VALUES OF J_{sc}, V_{OC}, EFFICIENCY, AND FILL FACTOR OF THE GAAS SOLAR CELLS GROWN AT VARIOUS GROWTH RATES

GR. (μm/h)	$J_{sc}/J_{sc-mesa}$ (mA/cm^2)	V_{oc} (V)	FF	η/η_{mesa} (%)
20	19.65/13.54 (0.229/0.158)	1.008 (0.002)	0.849 (0.006)	16.83/11.60 (0.263/0.181)
60	19.82/13.67 (0.132/0.091)	1.008 (0.002)	0.838 (0.012)	16.77/11.56 (0.239/0.165)
80	19.34/13.33 (0.146/0.100)	1.014 (0.002)	0.859 (0.007)	16.83/11.60 (0.223/0.154)

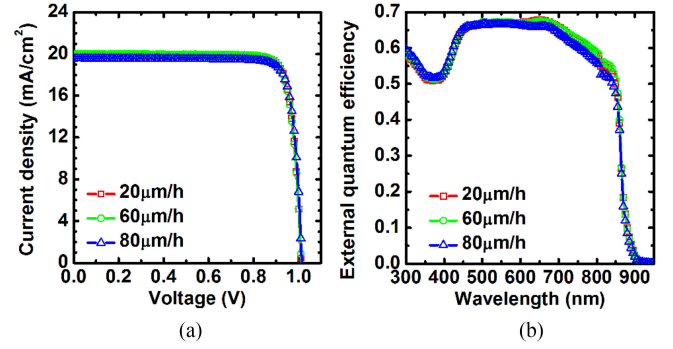
Fig. 8. (a) *I–V* characteristics under AM 1.5 illumination. (b) EQE spectra of the best GaAs solar cells in the fabrication batches grown at 20, 60, and 80 μm/h without ZnS/SiO$_2$ ARC evaluated using the effective area of 0.032 cm^2.
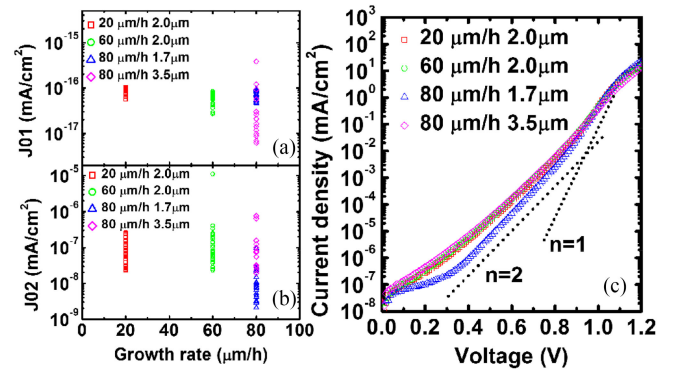

Fig. 9. (a) Dark *I–V* characteristics. (b) Distribution of J_{01} component (c) Distribution of J_{02} component of the GaAs solar cells with 2.0-μm-thick base grown at 20 and 60 μm/h, 1.7-μm-thick and 3.5-μm-thick base grown at 80 μm/h.

of 0.032 cm^2) with 2-μm thick base grown at various growth rates without ARC. Although there were 28 cells processed from each GaAs p-n wafer, the fabrication batch with 60 and 80 μm/h growth had two solar cells exhibiting relatively low V_{oc}, approximately 0.5–0.6 V, most likely because of fabrication failure. Thus, they were omitted from this distribution analysis. The average values of J_{sc}, V_{oc}, FF, and efficiency of the GaAs solar cells without ARC grown at various growth rates are summarized in Table II. On the basis of a standardized methodology, J_{sc} and η, evaluated by using the mesa area (0.047 cm^2), are also given in Table II denoted with "mesa" subscript. The standard deviation values of each data are also given in the brackets. The increase in the growth rate from 20 to 60 μm/h did not degrade the current density of the GaAs solar cells. However, the solar cell grown at the highest rate had a little bit lower J_{sc}. In contrast, this sample had the highest V_{oc} and FF. It is known that, if the efficiency of a GaAs thin-film solar cell is limited by Shockley–Read–Hall (SRH) recombination, V_{oc} is degraded with increasing base thickness [29]. Although on-substrate GaAs cells are different from thin-film PV, the relationship between V_{oc} and base thickness can potentially be explained by the same reason. Hence, the thinnest base layer of the 80 μm/h sample can be responsible for the enhancement of V_{oc}. Compensating for the lower current with better V_{oc} and FF, the efficiency of 80 μm/h solar cell was comparable with that of the other two samples. The *I–V* characteristics and EQE spectra of the most efficient GaAs solar cells in the fabrication batches grown at 20, 60, and 80 μm/h without ARC are evaluated using the effective area of 0.032 cm^2 and plotted in Fig. 8(a) and (b), respectively. The EQE spectra of all samples are almost identical at the short wavelength range and start to drop toward longer wavelengths at around 650 nm. This EQE degradation is most likely ascribed to insufficient light absorption in the 2-μm-thick bases. It is interesting that the 80 μm/h grown sample had a stepper EQE drop at long wavelength range corresponding to a smaller J_{sc}. This is probably a result of insufficient light absorption due to the unintentionally thinner base in this sample. The recovery of EQE in this wavelength range will be shown in the following section when the thickness of the base was increased to 3.5 μm.

To further investigate this performance issue, the dark *I–V* characteristics of all GaAs solar cells are measured and compared. For comparison, the dark *I–V* curve of the solar cell with 3.5-μm-thick base grown at 80 μm/h was also evaluated.

In the two-diode equation, J_{01} (ideality factor, $n = 1$) represents injection/diffusion in the quasi-neutral region and interface recombination, while J_{02} ($n = 2$) corresponds to generation/recombination both in the bulk space-charge region and within the space-charge region exposed at the perimeter of the mesa [30], [31]. Fig. 9(a) and (b) are distributions of J_{01} and J_{02} components of the GaAs cells grown at various growth rates, respectively. The semilog plots of Fig. 9(c) show dark *I–V* characteristics for each growth rate chosen from the median J_{02} in Fig. 9(b). In Fig. 9(a), the J_{01} components seem to be independent of growth rate, however, the cells with the 3.5-μm-thick base grown at 80 μm/h exhibited a broader J_{01} distribution. Clearly in Fig. 9(c), the dark *I–V* curve of the 60 μm/h grown sample more or less overlaps with that of the 20 μm/h one, indicating that the recombination processes in these two samples are similar to each other. This is in good agreement with the overlapping EQE spectra for 20 and 60 μm/h samples in Fig. 8(b). Meanwhile, with a growth rate of 80 μm/h, the cells with 1.7-μm-thick bases exhibited lower J_{02} component in Fig. 9(b), in accordance with the steeper *I–V* slope in the voltage range of 0.4–0.8 V in Fig. 9(c). However, the cells with 3.5-μm-thick bases at the same growth rate showed *I–V* characteristics that are almost identical with the cells grown at 20 and 60 μm/h. A lack of systematic dependence of J_{02} on the growth rate may suggest that no significant degradation in crystal quality existed
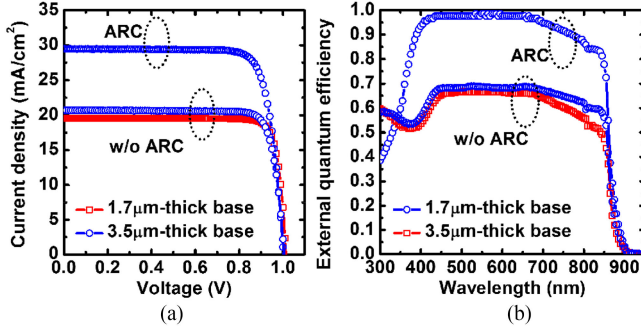
Fig. 10.   (a) I–V characteristics under AM 1.5G illumination. (b) EQE spectra of the GaAs solar cells with 1.7-μm-thick and 3.5-μm-thick base grown at 80 μm/h with and without ZnS/SiO$_2$ ARC evaluated using the effective area of 0.032 cm^2.

TABLE III
AVERAGE AND STANDARD DEVIATION VALUES OF J_{sc}, V_{oc}, FILL FACTOR, AND
EFFICIENCY OF THE GaAs SOLAR CELLS GROWN AT 80 μM/H WITH
DIFFERENT BASE THICKNESS

GR. (μm/h)	$J_{sc}/J_{sc\text{-}mesa}$ (mA/cm^2)	V_{oc} (V)	FF	η/η_{mesa} (%)
80 (1.7-μm)	19.34/13.33 (0.146/0.100)	1.014 (0.002)	0.859 (0.007)	16.83/11.60 (0.223/0.154)
80 (3.5-μm)	21.59/14.88 (0.135/0.093)	1.003 (0.004)	0.824 (0.013)	17.84/12.30 (0.385/0.265)
80 + ARC (3.5-μm)	29.36/20.23 (0.232/0.160)	1.003 (0.003)	0.801 (0.008)	23.59/16.25 (0.413/0.285)

in the base region as to clearly degrade dark I–V curve of the cells in the growth rate range from 20 to 80 μm/h.

The I–V curves and EQE spectra of 80 μm/h grown 1.7-μm-thick and 3.5-μm-thick base solar cells are plotted in Fig. 10(a) and (b), respectively. Obviously, the J_{sc} of the thicker base cell increased because of enhanced light absorption, ascribed to the higher EQE response at long wavelength ranges. An estimation of light absorbance using the Beer–Lambert law with GaAs parameters taken from [32] showed that almost 100% of light can be absorbed in this 3.7-μm-thick GaAs (0.2-μm emitter + 3.5-μm base). However, the EQE degradation at the wavelength range longer than 650 nm is still visible, possibly due to the failure in the collection of minority holes because the base thickness exceeds the carrier diffusion length. The average and standard deviation values of J_{sc}, V_{oc}, FF, and efficiency of each 80 μm/h solar cell batch are summarized in Table III. The FF of 3.5-μm-thick base sample with ARC was noticeably small, and consequently limited the cell efficiency to 23.6% (16.3% on the basis of a mesa area). The series resistance was considered as a factor that degraded the FF of this cell.

D. Discussions

In this paper, the relationship between the growth rate and performance of GaAs solar cell could not be evaluated clearly. Obviously, GaAs layers grown at 80 μm/h should contain some amount of crystal imperfection because V_{oc} decreased as the base thickness increased at this growth rate. However, the dependence

of growth rate on defect density could not be quantitatively extracted and compared. The first reason is that the impact of growth rate was influenced by insufficient light absorption in the 2-μm-thick bases. This was evidenced by a drop in EQE response in the long wavelength range which was independent of growth rate. In addition, the structure containing a highly doped n-GaAs base layer results in a very short hole radiative lifetime, which makes the impact of SRH recombination unclear. The second reason is that the absolute efficiency of solar cell in this work is not optimum. A typical MOCVD grown GaAs p-n solar cell can achieve a V_{oc} of 1.03 to 1.06 V [28], [33]. The previous report of high-speed grown n-p GaAs solar cells could also reach 23.8% to 24.6% [17]. Hence, the performance of solar cells in this paper (V_{oc} ∼ 1.00 to 1.01 V) seems to be limited by factors other than the quality of the GaAs base layer. The last reason is the p-on-n structure in this paper. It seems plausible that the lower mobility of minority holes in the n-GaAs base may make a p-on-n device more robust against the increase in defect density. Previous reports have shown that the hole lifetime is less sensitive to the increase in the threading dislocation density in GaAs than the electron lifetime [34], [35].

In conclusion, the quality of 80 μm/h grown GaAs in this paper is acceptably good, where defects and traps do not substantially degrade the solar cell efficiency as compared with the growth rates of 20 and 60 μm/h. There are two issues for further investigation. The first one is how high can conversion efficiency be obtained from this p-n solar cell grown at a high growth rate, for example, 80 μm/h. Several technical papers report a V_{oc} gain of 20–30 mV and an efficiency enhancement in GaAs solar cells by inserting a hetero BSF layer [36], [37]. This convinces us that, by employing the combination of adequate base thickness and a better BSF layer to prevent minority carrier diffusion to the substrate, accompanied by better fabrication processes, the efficiency of 24%–25% can be obtained for the cells grown at 80 μm/h. The second topic is how much can the cost of a p-n GaAs be reduced. Let us focus on the material cost. In this study, approximately 10% of the supplied TMGa could be utilized for the growth of GaAs on 2-inch-wafers, and the value was much lower in the case of AsH$_3$. Several methods have been proposed to improve the material utilization efficiency, for example, increasing the wafer size, lowering the V/III ratio, and improving the growth conditions. Considering the V/III ratio issue, in this report, the V/III ratio as high as 40 has been utilized during the growth of GaAs at 60 and 80 μm/h. Such a high V/III ratio can plausibly be a reason for no degradation in the cell performance up to 80 μm/h. As previously discussed, the robustness of p-n GaAs solar cell against the defect density in n-GaAs base may allow growths of GaAs with a lower V/III ratio with negligible performance degradation [38]. The optimization between material cost and growth quality should be carefully investigated in more detail. Moreover, the growth conditions for PV cells at high growth rates are not fully optimized at this stage. In addition to gas flow channel, several possible parameters to control the boundary layer thickness are currently under investigation. The crystalline quality as well as material consumption can be certainly improved in the future. Nevertheless, we investigated the feasibility of extremely high

growth rate in MOVPE, and demonstrated its capability for low cost, high-efficiency PV applications.

IV. SUMMARY

In this study, the extremely high-speed GaAs growth of up to 90 μm/h by MOVPE was demonstrated, with slight saturation of the growth rate above 70 μm/h. The impact of growth rates was examined using GaAs p-n solar cells, of which the 2-μm thick n-GaAs base layers were grown at 20, 60, and 80 μm/h. No dependence was clearly observed between the growth rate and cell performance. At present, we cannot fully ignore the detrimental impact of high growth rate on solar cell performance because

1) light absorption is insufficient in 2-μm-thick bases;
2) the absolute cell efficiency is limited by other factors including the immaturity of the fabrication technology;
3) the p-on-n structure is relatively robust against the defects and traps in the base layer. Within such restrictions, the extent of defect density in 80 μm/h grown GaAs was not identified to be a critical issue since it did not significantly degrade the solar cell efficiency as compared with the ones grown at 20 and 60 μm/h. As the growth rate in this MOVPE reactor could be accelerated to 90 μm/h, which is fast enough for general PV structures, what is to be compromised among material cost, machine utilization time, and solar cell performance will be the next research topic. In addition, the improvement of material utilization efficiency, especially TMGa, requires in-depth investigation as it directly and mainly affects the costs of GaAs solar cells. It is hoped that the results of this study will contribute to cost reductions in III–V PV production by high-speed epitaxial growth.

REFERENCES

[1] R. R. King *et al.*, "Solar cell generations over 40% efficiency," *Prog. Photovolt., Res. Appl.*, vol. 20, no. 6, pp. 801–815, Apr. 2012.

[2] D. C. Law *et al.*, "Future technology pathways of terrestrial III-V multijunction solar cells for concentrator photovoltaic systems," *Sol. Energy Mater. Sol. Cells*, vol. 94, no. 8, pp. 1314–1318, Aug. 2010.

[3] Y. Ohshita *et al.*, "Novel material for super high efficiency multi-junction solar cells," *J. Cryst. Growth*, vol. 318, no. 1, pp. 328–331, Mar. 2011.

[4] F. Dimroth *et al.*, "Four-junction wafer-bonded concentrator solar cells," *J. Photovolt.*, vol. 6, no. 1, pp. 343–349, Jan. 2016.

[5] D. C. Law *et al.*, "Lightweight, flexible, high-efficiency III-V multijunction solar cells," in *Proc. IEEE 4th World Conf. Photovolt. Energy Conf.*, Waikoloa, HI, USA, 2006, pp. 1879–1882.

[6] T. Takamoto *et al.*, "Paper-thin InGaP/GaAs solar cells," in *Proc. IEEE 4th World Conf. Photovolt. Energy Conf.*, Waikoloa, HI, USA, 2006, pp. 1769–1772.

[7] R. R. King *et al.*, "Pathway to 40% efficient concentrator photovoltaics," in *Proc. 20th Eur. Photovolt. Sol. Energy Conf. Exhib.*, Barcelona, Spain, Jun. 2005, pp. 118–123.

[8] H. L. Cotal *et al.*, "III-V multijunction solar cells for concentrating photovoltaics," *Energy Environ. Sci.*, vol. 2, no. 2, pp. 164–192, Feb. 2009.

[9] R. K. Jones, J. H. Ermer, C. M. Fetzer, and R. R. King, "Evolution of multijunction solar cell technology for concentrating photovoltaics," *Jpn. J. Appl. Phys.*, vol. 51, no. 10S, Oct. 2012, Art. no. 10ND01.

[10] N. H. Karam *et al.*, "Recent developments in high-efficiency Ga$_{0.5}$In$_{0.5}$P/GaAs/Ge dual- and triple-junction solar cells: Steps to next-generation PV cells," *Sol. Energy Mater. Sol. Cells*, vol. 66, nos. 1–4, pp. 453–466, Feb. 2001.

[11] R. R. King *et al.*, "Advanced III-V multijunction cells for space," in *Proc. IEEE 4th World Conf. Photovolt. Energy Conf.*, Waikoloa, HI, USA, 2006, pp. 1757–1762.

[12] R. R. King *et al.*, "Metamorphic concentrator solar cells with over 40% conversion efficiency," in *Proc. 4th Int. Conf. Sol. Concentrators*, El Escorial, Spain, 2007, pp. 5–8.

[13] W. Guter *et al.*, "Current-matched triple-junction solar cell reaching 41.1% conversion efficiency under concentrated sunlight," *Appl. Phys. Lett.*, vol. 94, no. 22, Jun. 2009, Art. no. 223504.

[14] G. J. Bauhuis, P. Mulder, E. J. Haverkamp, J. C. C. M. Huijben, and J. J. Schermer, "26.1% thin-film GaAs solar cell using epitaxial lift-off," *Sol. Energy Mater. Sol. Cells*, vol. 93, no. 9, pp. 1488–1491, Sep. 2009.

[15] C. Ebert *et al.*, "Fast growth rate GaAs and InGaP for MOCVD grown triple junction solar cells," in *Proc. IEEE 35th Photovolt. Spec. Conf.*, Honolulu, HI, USA, 2010, pp. 002007–002011.

[16] K. J. Schmieder *et al.*, "Analysis of GaAs solar cells at High MOCVD growth rates," in *Proc. IEEE 40th Photovolt. Spec. Conf.*, Denver, CO, USA, 2014, pp. 2130–2133.

[17] K. J. Schmieder *et al.*, "Effect of growth temperature on GaAs solar cells at high MOCVD growth rates," *J. Photovolt.*, vol. 7, no. 1, pp. 340–347, Jan. 2017.

[18] S. Mazumder and S. A. Lowry, "The importance of predicting rate-limited growth for accurate modeling of commercial MOCVD reactors," *J. Cryst. Growth*, vol. 224, nos. 1/2, pp. 165–174, Apr. 2001.

[19] T. R. Omstead, P. M. Van Sickle, P. W. Lee, and K. F. Jensen, "Gas phase and surface reactions in the MOCVD of GaAs from triethylgallium, trimethylgallium, and tertiarybutylarsine," *J. Cryst. Growth*, vol. 93, no. 1, pp. 20–28, 1988.

[20] S. J. C. Irvine and A. J. Clayton, "The kinetics of parasitic growth in GaAs MOVPE," *J. Cryst. Growth*, vol. 300, no. 2, pp. 277–283, Mar. 2007.

[21] S. D. Hersee and J. M. Ballingall, "The operation of metalorganic bubblers at reduced pressure," *J. Vac. Sci. Technol. A*, vol. 8, no. 2, pp. 800–804, Mar./Apr. 1990.

[22] B. Mayer, C. C. Collins, and M. Walton, "Transient analysis of carrier gas saturation in liquid source vapor generators," *J. Vac. Sci. Technol. A*, vol. 19, no. 1, pp. 329–344, Jan./Feb. 2001.

[23] D. T. J. Hurle, "A comprehensive thermodynamic analysis of native point defect and dopant solubilities in gallium arsenide," *J. Appl. Phys.*, vol. 85, no. 10, pp. 6957–7022, May 1999.

[24] K. L. Schulte and T. F. Kuech, "A model for arsenic anti-site incorporation in GaAs grown by hydride vapor phase epitaxy," *J. Appl. Phys.*, vol. 116, no. 24, Dec. 2014, Art. no. 243504.

[25] T. F. Kuech and E. Veuhoff, "Mechanism of carbon incorporation in MOCVD GaAs," *J. Cryst. Growth*, vol. 68, no. 1, pp. 148–156, Sep. 1984.

[26] T. J. Mountziaris and K. F. Jensen, "Gas-phase and surface reaction mechanisms in MOCVD of GaAs with trimethyi-gallium and arsine," *J. Electrochem. Soc.*, vol. 138, no. 8, pp. 2426–2439, Aug. 1991.

[27] C. R. Abernathy and W. S. Hobson, "Carbon-impurity incorporation during the growth of epitaxial group III-V materials," *J. Mater. Sci. Mater. Electron.*, vol. 7, pp. 1–21, Feb. 1996.

[28] S. P. Tobin *et al.*, "Assessment of MOCVD- and MBE-growth GaAs for high-efficiency solar cell applications," *IEEE Trans. Electron. Devices*, vol. 37, no. 2, pp. 469–477, Feb. 1990.

[29] A. W. Walker *et al.*, "Impact of photon recycling on GaAs solar cell designs," *J. Photovolt.*, vol. 5, no. 6, pp. 1636–1645, Nov. 2015.

[30] P. D. DeMoulin, S. P. Tobin, M. S. Lundstrom, M. S. Carpenter, and M. R. Melloch, "Influence of perimeter recombination of high-efficiency GaAs p/n heteroface solar cells," *IEEE Electron Device Lett.*, vol. 9, no. 8, pp. 368–370, Aug. 1988.

[31] A. Belghachi and S. Khelifi, "Modelling of the perimeter recombination effect in GaAs-based micro-solar cell," *Sol. Energy Mater. Sol. Cells*, vol. 90, no. 1, pp. 1–14, Jan 2006.

[32] G. E. Jellison, "Optical functions of GaAs, GaP, and Ge determined by two-channel polarization modulation ellipsometry," *Opt. Mater.*, vol. 1, no. 3, pp. 151–160, Sep. 1992.

[33] S. M. Hubbard *et al.*, "Effect of vicinal substrates on the growth and device performance of quantum dot solar cells," *Sol. Energy Mater. Sol. Cells*, vol. 108, pp. 256–262, Jan. 2013.

[34] A. Jorio, L. Sellami, M. Aubin, and C. Carlone, "Effect of intrinsic defects on the electron mobility of gallium arsenide grown by molecular beam epitaxy and metal organic chemical vapor deposition," *J. Appl. Phys.*, vol. 91, no. 12, pp. 9887–9893, Jun. 2002.

[35] C. L. Andre *et al.*, "Impact of dislocation densities on n$^+$/p and p$^+$/n junction GaAs diodes and solar cells on SiGe virtual substrates," *J. Appl. Phys.*, vol. 98, no. 1, Jul. 2005, Art. no. 014502.

[36] P. D. Demoulin, M. S. Lundstrom, and R. J. Schwartz, "Back-surface field design for n$^+$p GaAs cells," *Sol. Cells*, vol. 20, no. 3, pp. 229–236, Apr. 1987.

[37] B. Galiana, I. Rey-Stolle, M. Baudrit, I. Garciaand, and C. Algora, "A comparative study of BSF layers for GaAs-based single junction or multijunction concentrator solar cells," *Semicond. Sci. Technol.*, vol. 21, pp. 1387–1392, Aug. 2006.

[38] H. Xu *et al.*, "Effect of low-V/III-ratio metalorganic vapor-phase epitaxy on GaAs solar cells," *Jpn. J. Appl. Phys.*, vol. 56, no. 8S2, Jul. 2017, Art. no. 08MC06.

Hassanet Sodabanlu was born in Bangkok, Thailand, on December 27, 1978. He received the B.Eng. degree from Chiang Mai University, Chiang Mai, Thailand, in 2001, and the M.Eng. degree from Chulalongkorn University, Bangkok, in 2005, both in electrical engineering, and the Ph.D. degree in electronic engineering from the University of Tokyo, Tokyo, Japan, in 2010.

Since 2010, he has been a Project Researcher with the Research Center for Advanced Science and Technology, University of Tokyo. His research interests include crystal growth by metalorganic vapor-phase epitaxy (MOVPE), quantum nanostructures, and multijunction solar cells.

Dr. Hassanet is a Member of the Japan Society of Applied Physics (JSAP).

Akinori Ubukata received the B.S. and M.S. degrees in electrical engineering from Science University of Tokyo, Tokyo, Japan, in 1989 and 1991, respectively, and the Ph.D. degree from the Tokyo University of Science, Tokyo, Tokyo, Japan, in semiconductor lasers using MOCVD in 2004.

He joined Taiyo Nippon Sanso Corporation (Nippon Sanso at the time) in 1991. He also studied as a Visiting Researcher with Tokyo Institute of Technology from 1993 to 1996. Since 1991, he has been working on the study of epitaxial growth of III–V compound semiconductors as well as developing reactor.

Kentaroh Watanabe received the B.S. degree from the Department of Physics, Hokkaido University, Hokkaido, Japan, in 2002, and the M.S. and Ph.D. degrees from the Department of Astronomy, University of Tokyo, Tokyo, Japan, in 2004 and 2007, respectively.

In 2007, he joined the Institute of Space and Astrophysical Science, Japan Aerospace Exploration Agency, Kanagawa, Japan, where he became a Researcher. In 2009, he joined the Research Center for Advanced Science and Technology, University of Tokyo, where he became a Project Assistant Professor. His current research interests include the ultrahigh-efficiency photovoltaic devices and metal-organic vapor phase epitaxy of III–V compound semiconductors.

Dr. Watanabe is a Member of Japan Society of Applied Physics (JSAP), the Astronomical Society of Japan (ASJ), and the International Society of Optics and Photonics (SPIE).

Takeyoshi Sugaya received the B.E., M.S., and Ph.D. degrees from Tsukuba University, Tsukuba, Japan, in 1989, 1991, and 1994, respectively.

In 1994, he joined the Electrotechnical Laboratory and was engaged in molecular beam epitaxy (MBE) growth and quantum devices of compound semiconductors. During 2000–2001, he was a Visiting Researcher with Arizona State University, where he worked on electron transport in quantum nanostructures. He is currently the team leader in Smart Stack Device Team, Research Center for Photovoltaics, National Institute of Advance Industrial Science and Technology (AIST), Tsukuba, where he is involved in the fabrication of high-efficiency multijunction solar cells using mechanical stacking.

Dr. Sugaya is a Member of the Japan Society of Applied Physics and the Institute of Electronics, Information and Communication Engineers.

Yoshiaki Nakano (S'81–M'87) received the B.E., M.S., and Ph.D. degrees in electronic engineering from the University of Tokyo, Tokyo, Japan, in 1982, 1984, and 1987, respectively.

He is a Professor with the Department of Electrical Engineering and Information Systems (EEIS), Graduate School of Engineering, University of Tokyo. He is also with the Research Center for Advanced Science and Technology, University of Tokyo. In 1984, he spent a year with the University of California, Berkeley, as an exchange student. In 1987, he joined the Department of Electronic Engineering, University of Tokyo, became an Associate Professor in 1992, a Professor in 2000, and the Department Head in 2001. He moved to RCAST, University of Tokyo, in 2002 as a Professor, and he served as the Director General with the center from 2010 to 2013. Then he moved back to the Engineering School to fill up the current professorship position with the Department of EEIS. Since 2010, he has also been serving as the Co-Director of Presidential Endowed Chair on Global Solar Plus Initiative attached direct to the University of Tokyo president office. In 1992, he was a Visiting Associate Professor with the University of California, Santa Barbara. He has authored and coauthored more than 250 refereed journal publications and more than 500 international conference papers, and he holds 40 patents. His research interests include fabrication technologies of semiconductor optical modulators/switches, monolithically integrated photonic circuits, and high-efficiency solar cells.

Dr. Nakano was an elected member of the Board of Governors of IEEE LEOS, and directors of the Japan Society of Applied Physics (JSAP), the Editor-in-Chief of Applied Physics Express (APEX) and *Japanese Journal of Applied Physics*, and a member of the Board of Directors of the Japan Institute of Electronics Packaging. He is currently the President of Electronics Society, Institute of Electronics, Communication, and Information Engineers, the Chairman of the Optoelectronics Technology Trend Research Committee of the Optoelectronics Industry and Technology Development Association, and the Optical Interconnect Standardization Committee of Japan Electronics Packaging and Circuits Association. He is an Associate Member of the Science Council of Japan. He served as the Project Leader of Japanese National Project on "Photonic Networking Technology" organized by the Ministry of Economy, Trading, and Industry (METI), and as the Project Leader of SORST Program on "Nonreciprocal Semiconductor Digital Photonic Integrated Circuits and their Applications to Photonic Networking" sponsored by Japan Science and Technology Corporation. He is currently the project leader of METI National R&D Project on "Post-Silicon Solar Cells for Ultra-High Efficiencies". He was the recipient of the 1987 Shinohara Memorial Prize from the IEICE, the 1991 Optics Paper Award from the JSAP, the 1997 Marubun Science Prize, the 2007 Ichimura Prize, the 2007 IEICE Electronics Society Award, the 2007 Sakurai Medal from the OITDA, and the Prime Minister Award in Collaborative Research between Academia and Industry in 2007.

Masakazu Sugiyama received the B.E., M.S., and Ph.D. degrees in chemical systems engineering from the University of Tokyo, Tokyo, Japan, in 1995, 1997, and 2000, respectively.

He is a Professor with the Research Center for Advanced Science and Technology, University of Tokyo. During 1997–2000, he was a Research Fellow of the Japan Society for the Promotion of Science (JSPS). In 2000, he became a Research Associate with the Department of Chemical System Engineering, University of Tokyo. In 2002, he joined the Department of Electronic Engineering as a Lecturer. He became an Associate Professor in 2005. He was promoted to an Associate Professor and a Professor in 2006 and 2016, respectively. His current research interests include high-efficiency III–V semiconductor solar cells, photoelectrochemical cells, quantum nanostructures, the crystal growth by metalorganic vapor-phase epitaxy (MOVPE), and nano-micro fabrication processes, including photon-trapping mechanism as an efficiency booster for solar cells. He authored and coauthored more than 130 refereed journal publications and more than 140 international conference papers, and he holds 15 patents.

Dr. Sugiyama is a member of Japan Society of Applied Physics, the Society of Chemical Engineers, Japan, and Japanese Association for Crystal Growth. He was the recipient of the Young Investigator Researcher Award from SCEJ.